Available online at www.sciencedirect.com
SCIENCE DIRECT®
ELSEVIER
Continental Shelf Research 24 (2004) 317–335
CONTINENTAL SHELF RESEARCH
www.elsevier.com/locate/csr

Suspension of coarse and fine sand on a wave-dominated shoreface, with implications for the development of rippled scour depressions

Malcolm O. Green[a,*], Christopher E. Vincent[b], Arthur C. Trembanis[c]

[a] *National Institute of Water and Atmospheric Research, P.O. Box 11-115, Hamilton, New Zealand*
[b] *School of Environmental Sciences, University of East Anglia, Norwich NR4 7TJ, UK*
[c] *Virginia Institute of Marine Science, Gloucester Point, VA 23062, USA*

Received 18 June 2003; received in revised form 29 October 2003; accepted 18 November 2003

Abstract

Measurements of waves, currents and sediment suspension from a 35-day deployment of three instrumented tripods on the wave-dominated shoreface off Tairua Beach, New Zealand, are presented. Two tripods were deployed at 22-m depth, one within a coarse-sand rippled scour depression (RSD), and the other nearby on the surrounding, relatively featureless fine-sand plain. A third tripod was deployed at 15-m depth, also on fine sand. To distinguish between suspended fine and coarse sand at each site, a method of simultaneously inverting two-frequency acoustic backscatter data was applied.

Background, long-period swell was interrupted by two 6-day periods of high waves. At the 15-m/fine-sand site, only fine sand appeared in suspension. However, at the 22-m/fine-sand site, coarse sand appeared in suspension together with fine sand when the waves were highest. This suggests that coarse sand resuspended from the RSD can be dispersed on the adjacent fine-sand plain, at least along the same isobath. At the RSD, there was no coarse sand in suspension under background swell, but there was a fine-sand "washload", presumably advected from the surrounding fine-sand plain, even though the coarse bed sediment in the RSD itself was not in motion. Under high waves, both fine and coarse sands were in suspension over the RSD. The fine sand appeared again as a washload, but the coarse sand was confined relatively close to the bed in accordance with a sediment diffusivity that decreased linearly with elevation above the bed.

Measurements of fine-sand reference concentration over both fine-sand beds (15 and 22-m depth) plot against wave-induced skin friction in one cluster under the background swell and in another cluster under the high waves, which suggests a change in bedforms, possibly to a hummocky bed, that is related to wave conditions and that alters the suspension dynamics. The coarse-sand reference concentrations over the RSD fall into the "hummocky cluster", which supports this interpretation.

The fine-sand washload is indicative of an unfavourable settling environment over the RSD, which could constitute a positive feedback that causes RSDs to self-organize from initial perturbations. Under high waves, the suspended-sediment load impinging from the surrounding plain will be high, but turbulence will also be more energetic on the RSD, thus more effectively inhibiting deposition. Under low waves, deposition may be less inhibited on the RSD, but the suspended-sediment load arriving from the surrounding fine-sand plain will also be lower. Thus, the fine-sand deposition rate on the RSD will be small, even though conditions are more favourable for settling. Modelling could be expanded to consider the balance between inhibition of settling and tendency for burial by the sediment load that

*Corresponding author. Fax: +64-7-856-0151.
E-mail address: m.green@niwa.co.nz (M.O. Green).

0278-4343/$ - see front matter
doi:10.1016/j.csr.2003.11.002

impinges from the area surrounding an RSD, and the way wave climate and water depth might mediate the basic self-organization process. Escape of coarse sand from RSDs under high waves may seed the growth of new RSDs.

Keywords: Sediment transport; Resuspension; Nearshore dynamics; Shoreface; Rippled scour depression; Self-organization

1. Introduction

Field measurements tend to reinforce a one-dimensional point of view that links local boundary-layer and sediment dynamics with the local seabed configuration (bedforms, sediment type) and local driving forces (waves, currents) (e.g., Cacchione and Drake, 1982; Wright et al., 1986, 1991; Huntley and Hanes, 1987; Vincent et al., 1991; Madsen et al., 1993; Green et al., 1995; Williams et al., 1999; Storlazzi and Jaffe, 2002). However, it is the sediment-flux divergence that drives evolution of geomorphology, not the local dynamics per se. On the shoreface, which is the zone of shoaling waves between the breakpoint and the edge of the inner shelf (Niedoroda et al., 1984), there is a marked spatial gradient in driving forces related primarily to change in water depth and the effect that that has on penetration of wave-orbital motions down to the bed. There may also be less predictable and more localised variability related to non-uniform bed sediments, including "rippled scour depressions" (RSDs), which are persistent patches of prominently rippled coarse sand within relatively featureless fine-sand plains (Cacchione et al., 1984; Hunter et al., 1988; Thieler et al., 1995). The shoreface, with its mix of large-scale gradients in forcing and more localised variability in seabed characteristics, is a particularly good setting for studying how broadscale sediment-flux divergence emerges from spatially variable dynamics. The first step is to determine how the dynamics varies with substrate and depth. This understanding can then be codified in models to investigate spatial patterns of sediment transport and associated sediment-flux divergence. At least two different modelling approaches are available (which could be argued to occupy the opposite ends of the one continuum): solution of the partial differential equations that describe momentum and mass (sediment) conservation, and construction of "abstract" models based on scale-dependent, usually simplified equations (or "rules"). The aim of this paper is to determine how time-averaged suspended-sediment concentration (SSC) varies over the shoreface. Specifically, we compare measurements from three locations that encompass different combinations of water depth and seabed configuration.

We recognise that by focusing on the properties of the time-averaged suspension, we are discarding information that might relate to any suspended-sediment flux that arises by "flux coupling" (Jaffe et al., 1985). Although flux coupling at gravity- and infragravity-wave frequencies does occur under shoaling waves (e.g., Hanes and Huntley, 1986), field measurements have confirmed that advection of the mean suspension field by the mean current is typically the dominant transport term seaward of the surfzone (e.g., Green et al., 1995). Nevertheless, flux coupling might perturb or modulate the transport field in significant ways (e.g., Storlazzi and Jaffe, 2002), and might therefore play a part in shaping shoreface morphology.

The data are from a 35-day deployment of three instrumented tripods on the shoreface off Tairua Beach, which is a 1.2-km-long baymouth barrier on the steep and rocky eastern coastline of the Coromandel Peninsula, which in turn is on the eastern coast of the North Island of New Zealand (Fig. 1). Tripods *Kelly* and *Alice* were both deployed at 22-m depth off Tairua Beach, but *Kelly* was located within a coarse-sand RSD with prominent ripples, whereas *Alice* was located on the relatively featureless fine-sand plain that surrounded the RSD (Fig. 2). The third tripod, *Bud*, was also located on the fine-sand plain, but at 15-m depth. Table 1 provides a summary of the depth and seabed characteristics at each tripod location.

Hume et al. (2003) found that the coarse-sand floors of the RSDs at Tairua are underlain by fine

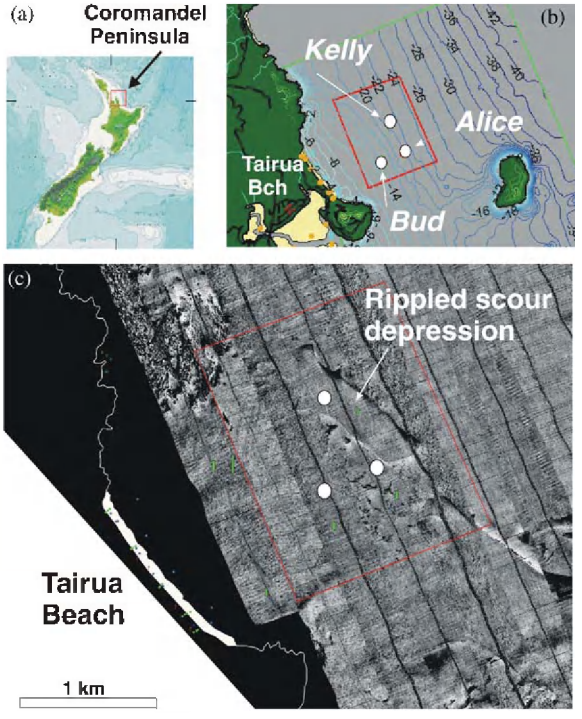

Fig. 1. Tripod locations: (a) study site in New Zealand context: (b) bathymetry of shoreface and inner shelf off Tairua Beach, showing tripod locations; and (c) sidescan-sonar image of shoreface and inner shelf off Tairua Beach, showing tripod locations and the RSD where *Kelly* was located. Darker colours denote higher (sidescan) acoustic backscatter.

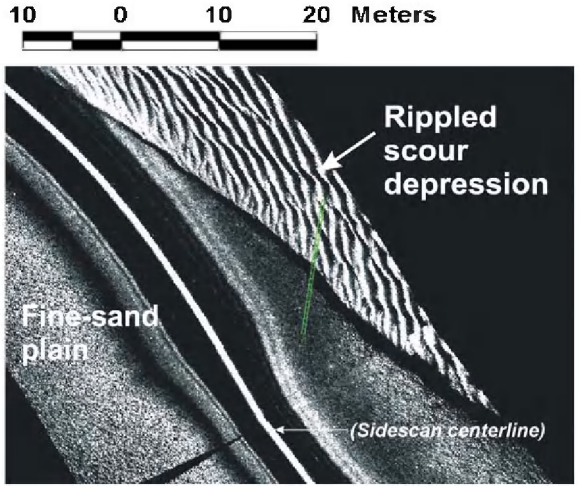

Fig. 2. Sidescan-sonar image showing coarse-sand RSD with prominent ripples, and the surrounding, relatively featureless fine-sand plain. Darker colours denote higher (sidescan) acoustic backscatter.

Table 1
Depth and seabed characteristics at each tripod location

	Tripod *Kelly*	Tripod *Alice*	Tripod *Bud*
Depth (m)	22	22	15
Substrate	RSD	Fine-sand plain	Fine-sand plain
Mean grain size (mm)	0.75	0.22	0.22
Fairweather bedform height/length (cm)	35/125	5/20	3/16

sand; also, coarse-sand lenses are interbedded with fine sand. Hunter et al. (1988) described a similar situation from southern Monterey Bay (California), and suggested that RSDs are best explained as lag deposits in areas of localised scour. Various hydrodynamic forcings have been proposed for initiating these features on open shelves, including: rip currents during storms (Reimnitz et al., 1976); waves and currents steered in the vicinity of bathymetric irregularities; wind-driven coastal currents, particularly downwelling bottom currents (Cacchione et al., 1984); and wave-driven currents (Karl, 1980).

Recently, Murray and Thieler (2003) advanced an alternative explanation for the origin and growth of RSDs based on a morphodynamic instability driven by sediment–flow feedbacks. Interactions between flow and sediment transport that are driven by grain-size sorting and resultant variations in bed roughness lead to segregation of coarse and fine sediment, albeit, initially, at a scale much smaller than the scale of natural RSDs. However, subsequent interactions between flow and growing finite-amplitude features as well as merging of features that are growing at different rates may then produce patterns with scales and shapes that are similar to natural features. This school of thinking, known as "self-organization" (in the sense that intial perturbations grow or "organize" to become the features themselves), differs fundamentally from the school that postulates a passive sediment bed that is imprinted by a spatial pattern of hydrodynamic forcing. To emphasise the distinction, Murray and Thieler suggested the term "sorted bedforms" be used to name the features that are otherwise known as

"RSDs". The flow–sediment interaction hypothesised by Murray and Thieler to be at the heart of the self-organization is a winnowing process. In essence, increased energy and scales of turbulence over coarse-sediment domains inhibit deposition of fine suspended sediment locally. The fine sediment prevented from settling on the coarse domain is advected downstream until it encounters an area of fine bed sediment, where turbulence is relatively less energetic and deposition is favoured. Thus, fines are preferentially deposited in areas where fines are already in the seabed. This positive feedback will cause any initial perturbation in the distribution of coarse and fine grains on the seabed to grow. The analysis of the Tairua dataset presented herein will shed some light on this process.

2. Study area

The continental shelf off the Coromandel Peninsula is 20–30 km wide (Bradshaw et al., 1994). Tides are semidiurnal with a spring range of $\sim$1.5 m. Tidal currents are generally weak ($< \sim$10 cm/s at 100 cm above the bed), except at the mouths of tidal inlets and in the vicinity of offshore islands. The Coromandel coast is a lee shore (dominant wind direction west to southwest) that has been classified by Carter and Heath (1975) as a storm-dominated coast. The wave climate is a mix of locally generated sea waves and distantly generated swell. Highest swell is associated with cyclones that leave the tropics and pass to the east of New Zealand. Average significant wave height is 0.9 m (swell associated with cyclones up to 7 m) and average period is 5.8 s (up to 13 s) (Gorman et al., 2003).

The offshore profile at Tairua is convex between depths of 8 and 25 m, beyond which it flattens. Bed sediments are primarily unimodal fine sand (mean grain size 0.22 mm), but with areas of poorly sorted coarse sand (mean grain size 0.75 mm) in localised RSDs. Hume et al. (2003) identified five facies on the Tairua shoreface and inner shelf. (1) Fine-sand plain: This facies is surmounted by small, symmetrical wave ripples, as well as shallow pits and humps that might be remnants of hummocky bedforms after reworking by waves and bioturbation. (2) Outcrop-related RSDs: These are bands of poorly sorted gravelly sands with large ripples adjacent to and in contact with reef outcrops. (3) Nearshore shore-normal RSDs: These are finger-like ribbons of coarse sands in shallow depressions that run normal to shore in depths of 6–16 m. They are typically surmounted by large symmetrical wave ripples. (4) Offshore shore-parallel RSDs are coarse sands in shallow depressions that run parallel to shore in depths of 18–26 m, typically covered with large symmetrical wave ripples. (5) Offshore shore-oblique RSDs are coarse, rippled sands in depressions in water depths $>$30 m. These appear to be associated with low-amplitude sand ridges.

3. Data

Each tripod had a pressure sensor for measuring waves; current meters for measuring turbulence, mean currents and wave-orbital currents; and a multi-frequency acoustic backscatter sensor (ABS) for measuring SSC close to the bed. Table 2 shows

Table 2
Sampling details

	Tripod *Kelly*	Tripod *Alice*	Tripod *Bud*
	$\Delta f, BD, IBB/z$	$\Delta f, BD, IBB/z$	$\Delta f, BD, IBB/z$
Pressure	1, 900, 60/200	4, 512, 60/120	1, 900, 60/200
EMCM	1, 900, 60/115	4, 512, 60/64	1, 900, 60/76
ADV	5, 300, 60/53, 64	—/—	5, 300, 60/24, 41
	$\Delta f, BD, IBB/z$	$\Delta f, BD, IBB/z$	$\Delta f, BD, IBB/z$
	$F1, F2, F3$	$F1, F2, F3$	$F1, F2, F3$
ABS	2.5, 300, 60/67	5, 600, 60/109	2.5, 300, 60/67
	0.92, 3.55, —	1.08, 1.97, 4.38	1.09, 1.98, 4.97

Δf is sampling frequency in Hz. *BD* is burst duration in s. *IBB* is interval between bursts in min. z is elevation of sensor above bed in cm. "EMCM" denotes two-axis, 3.8-cm diameter, Marsh–McBirney electromagnetic current meter (measuring two horizontal components of flow). "ADV" denotes three-axis Sontek acoustic Doppler velocimeter (measuring two horizontal components and the vertical component of flow). "ABS" denotes multi-frequency acoustic backscatter sensor, where $F1$, $F2$ and $F3$ are operating frequencies in MHz.

sampling details. Wave statistics were estimated from pressure and current data as follows.

Significant wave-orbital speed at the bed, U_{sig}, was calculated using linear wave theory as:

$$U_{sig} = \left(\int_{1/30\ s^{-1}}^{1/2\ s^{-1}} \Gamma_U(f)\, df \right)^{1/2} \frac{2}{\cosh[k(z_C + h)]}, \quad (1)$$

where $\Gamma_U(f)$ is the power spectrum of $U(z_C, t)$, which is the current-speed time series at elevation z_C above the bed; f is frequency; the limits of integration correspond to the gravity-wave range of frequencies; and k is the linear-theory wavenumber corresponding to mean water depth h (calculated from pressure data after correcting for a nominal atmospheric pressure and assuming a nominal seawater density) and mean spectral period T (also calculated from the pressure data, using the definition of Longuet-Higgins, 1975). Significant wave height, H_{sig}, was estimated as:

$$H_{sig} = (U_{sig} T/\pi)\sinh(kh). \quad (2)$$

The ABS ensonifies a 120-cm long cone of water and registers the backscattered acoustic pressure from 1-cm thick bins down the entire length of the cone. SSC in each 1-cm bin is inferred from ABS echo data by solving an equation that relates SSC, echo intensity, a size-dependent term that describes the amount of energy back-scattered from the sediment (form function), range from transducer and a system-specific calibration constant (e.g., Thorne et al., 1991; Thorne and Hanes, 2002). With one operating frequency, the grain-size distribution of suspended sediment needs to be specified in order to evaluate each term in the equation and solve for SSC. Furthermore, the grain-size distribution is assumed to be constant through time and across the sounding range. For multi-frequency ABS units, which were used in this study, backscatter data from two or more frequencies can be combined to calculate concentration and suspended-particle size (Crawford and Hay, 1993). However, the inversion can be "noisy" and only permits a single size at each range and time. In this study, an assumption was made: both the coarse sand found in the RSDs (mean grain size 0.75 mm) and the fine sand that composes the surrounding plain (mean grain size 0.22 mm) will supply the suspended-sediment field over the shoreface. With this assumption, it was possible to develop a simultaneous two-frequency data inversion to partition the SSC into these two size components.

Burst-averaged SSC profiles $\bar{C}_{fine}(r)$ and $\bar{C}_{coarse}(r)$ were obtained by applying the two-frequency data inversion to the echo data, where r is range of bin from transducer face, "fine" denotes the 0.22-mm particle size and "coarse" denotes the 0.75-mm particle size. Each ABS was positioned such that the seabed surface would intersect the ensonifying cone at some nominal range. The actual range from the transducer of the bed surface, r_{bed}, is readily discernable as a distinct break in slope in $\bar{C}(r)$ when plotted in $\log_{10}(\bar{C}) - r$ space (Green and Black, 1999). r_{bed} for each burst was estimated by locating the break of slope in $\bar{C}_{fine}(r)$, and r_{bed} thus determined was used in the transformation $z = r_{bed} - r$ to convert $\bar{C}_{fine}(r)$ and $\bar{C}_{coarse}(r)$ to $\bar{C}_{fine}(z)$ and $\bar{C}_{coarse}(z)$, respectively.

The dual-frequency data inversion, as applied in this study, yields only burst-averaged concentration profiles (fine and coarse particles), which precludes any analysis of intra-burst suspension processes (e.g., intermittency due to interaction of wave-orbital motions with bedforms). To enable at least a qualitative description of such processes, the single-frequency inversion of acoustic backscatter data employed by Green (1999) and Green and Black (1999), which requires specification of a single particle size and which yields estimates of "instantaneous" concentration (i.e., at the sampling frequency), was also used. For this, a mean grain size of 0.22 mm was assumed (fine sand), hence the inversion of each burst of echo data results in an estimate of $C_{fine}(r, t)$, where t is time and the interval between points and points per burst can be seen in Table 2. We note that $(1/BD)\int_0^{BD} C_{fine}(r, t)\, dt$ (where BD is the burst duration and $C_{fine}(r, t)$ is from the single-frequency inversion) is not identical to $\bar{C}_{fine}(r)$ from the dual-frequency inversion, although they will be very similar when no coarse sand is in suspension.

4. Results

Fig. 3 shows wave statistics estimated from the *Alice* data. Background, long-period Pacific Ocean swell (H_{sig} 50–100 cm) was interrupted by two 6-day periods of high waves ($H_{sig} > 200$ cm). During those times, U_{sigb} exceeded 60 cm/s. U_{64}, the mean current speed measured at 64 cm above the bed, was small relative to U_{sigb}. During the period of high waves, sediment was in suspension at all three sites (methodology described below). Under the background swell, sediment was in suspension continuously at the 15-m/fine-sand site (*Bud*), less so at the 22-m/fine-sand site (*Alice*), and occasionally at the 22-m/coarse-sand RSD (*Kelly*).

4.1. Overview of suspension patterns

Suspension was generally intermittent at two scales: the wave-group and the individual-wave scales (Fig. 4). Forced long waves associated with wave groups can cause a flux coupling (Jaffe et al., 1985) at the infragravity scale, which results in net offshore sediment transport (e.g., Shi and Larsen, 1984; Villard et al., 1999; Green and MacDonald, 2001). Intermittency at the individual-wave scale is usually attributable to the orderly ejection of sediment-laden vortices from the bed, which is caused by interaction between wave-orbital motions and seabed ripples (e.g., Bagnold, 1946; Sleath, 1982; Hanes and Huntley, 1986). The data in Fig. 4, which are typical of energetic conditions, show that intermittency at the individual-wave scale is accentuated at both deep sites relative to the shallow site. Furthermore, vortex entrainment is more "pronounced" (i.e., sediment in suspension for a greater proportion of the time; more

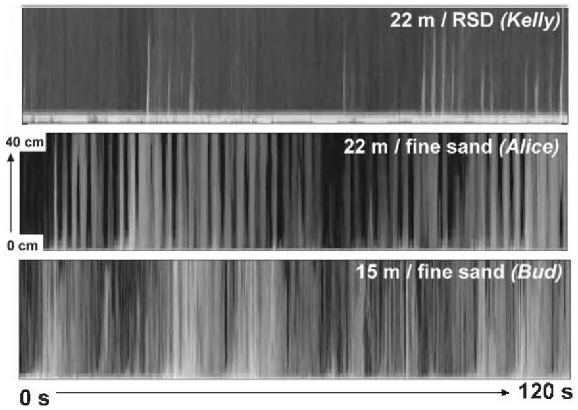

Fig. 4. Three bursts of suspension data ($C_{fine}(z,t)$ from the single-frequency data inversion); different locations, same time. The grayscale is the same for each plot; black represents zero SSC and white represents high SSC. The seabed is at the bottom of each panel.

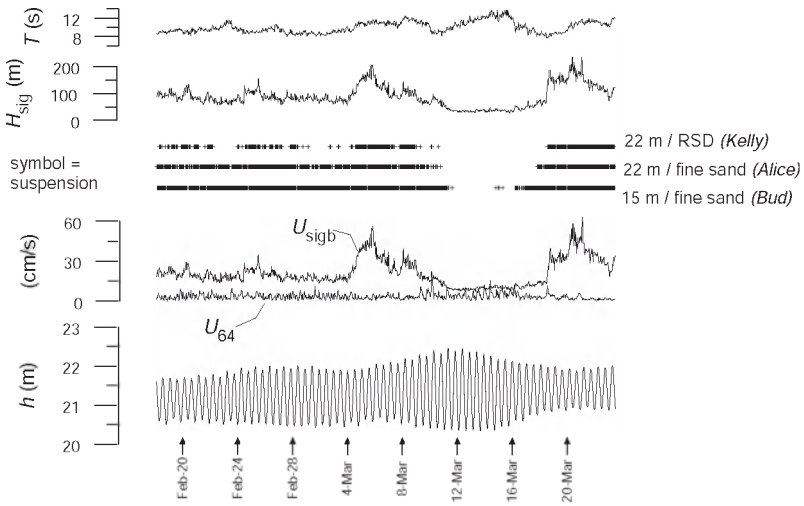

Fig. 3. Waves and currents during the experiment measured at the *Alice* site and symbols showing whether sediment was in suspension at each of the three tripod sites.

sediment in suspension; suspension to higher levels in the flow) over the fine-sand plain compared to over the RSD at the same depth. These differences suggest that net sediment flux arising from flux coupling at the individual-wave scale will vary strongly with both depth and substrate.

A kind of "washload" suspension was frequently observed over the RSD. Washload was characterized by virtually zero intermittency at both wave-group and individual-wave scales. Furthermore, SSC in the washload was virtually uniform to at least 1 m above the bed. The significance of this observation will be explored.

4.2. Suspension type and composition

The ABS data were inspected to classify each burst into one of four categories: "no suspension", "intermittent suspension" (sediment in suspension for $< \sim 15\%$ of the time during a burst), "full suspension" (sediment in suspension for $> \sim 15\%$ of the time of a burst), and "washload". The classification was performed by inspecting data plots of the type shown in Fig. 4. The category "no suspension" was easily identifiable as such. The difference between intermittent suspension and full suspension was discerned from a rough estimate of the percentage of time sediment clouds were present during the burst. Washload was recognised on a subjective basis as described above (approximately zero intermittency; SSC approximately uniform to at least 1 m above the bed). The results of the classification are shown in Fig. 5, where U_{crit} is the critical wave-orbital speed at the bed for initiation of suspension estimated from Komar and Miller (1975). U_{crit} for the fine-sand plain was based on grain size $D = 0.22$ mm and 0.75 mm was used for the coarse sand in the RSD. Following Green (1999), Komar and Miller's equation for U_{crit} was evaluated using significant wave height and mean spectral period.

Also shown in Fig. 5 is the grain size that was in suspension, either coarse (0.75 mm) and/or fine (0.22 mm). The presence of coarse and fine sand was inferred from $\bar{C}_{coarse}(z)$ and $\bar{C}_{fine}(z)$, respectively: when the burst-averaged concentration was at the background noise level of the ABS ($\sim 0.1\,mg\,l^{-1}$) at all elevations above the bed, the corresponding component was deemed not to be present in suspension.

At both fine-sand sites (*Alice*, 22-m depth, and *Bud*, 15-m depth), U_{crit} based on $D = 0.22$ mm effectively divides no suspension from full suspension. During full suspension at the fine-sand/15-m site there was never any coarse sand in suspension. However, at the fine-sand/22-m site, which is near the RSD also at 22-m depth, coarse sand appeared in suspension with the fine sand when the waves were highest. This suggests that coarse sand resuspended from the RSD by high waves can be dispersed on the adjacent fine-sand plain at least along the same isobath, and possibly farther. An alternative explanation for the source of the suspended coarse sand that appears over the fine-sand plain at 22-m depth under high waves is that it is local, which is not likely, for two reasons. Firstly, the surficial sediments of the fine-sand plain are very well sorted (Hume et al., 2003) and, hence, could not act as a significant source of coarse sand. Secondly, the lenses of coarse sand that are known to be buried beneath the fine-sand plain are, at a minimum, 30–40 cm below the sediment surface (Hume et al., 2003), which is at least an order of magnitude greater than the "erosion depth" (estimated as the thickness of settled sediment corresponding to the total suspended-sediment load). Hence, exhumation of buried coarse material is unlikely.

Intermittent suspension at both fine-sand sites tends to straddle U_{crit}, with more intermittent-suspension bursts occurring below U_{crit} than above. A possible explanation is that wave groupiness tends to bias U_{sigb} estimates toward low values, but the ABS still captures the intermittent suspension. At both fine-sand sites, only fine sand was present in intermittent suspension.

At the RSD site (*Kelly*, 22-m depth), U_{crit} based on $D = 0.75$ mm effectively divides no suspension from full suspension. Both coarse sand and fine sand were always present during full suspension. In contrast, the washload, which tended to occur at times when U_{sigb} was greater than U_{crit} based on $D = 0.22$ mm but less than U_{crit} based on $D = 0.75$ mm (Fig. 6), was always composed entirely of fine sand. This suggests that the fine

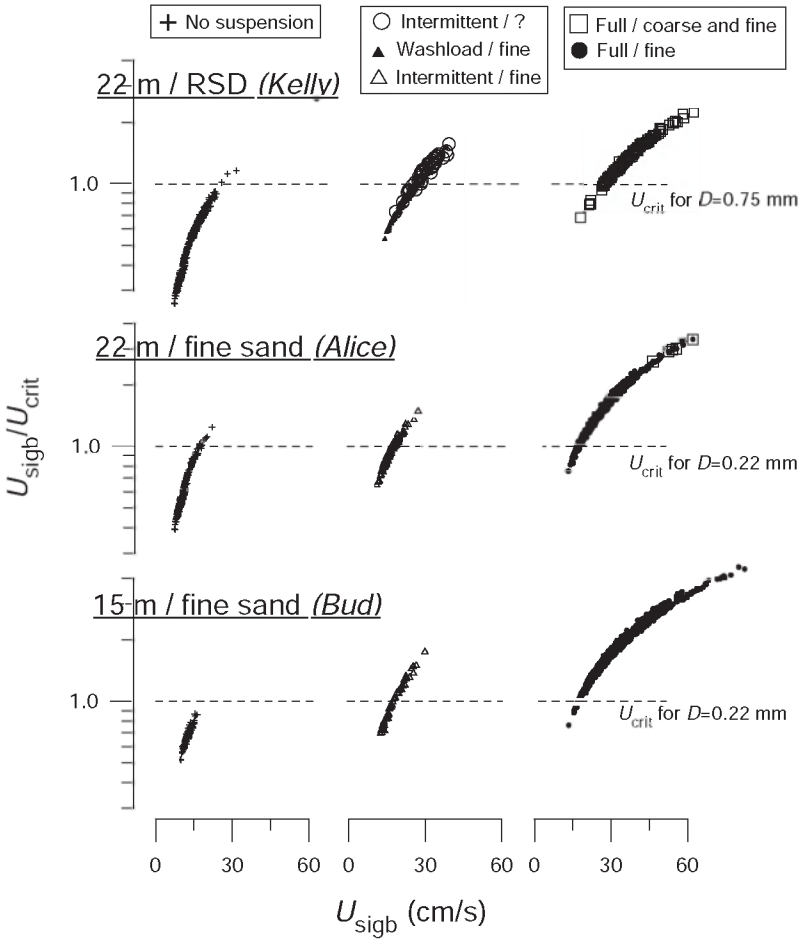

Fig. 5. Bursts classified by suspension type (none, intermittent, full, washload) and grain size (coarse, fine) in suspension.

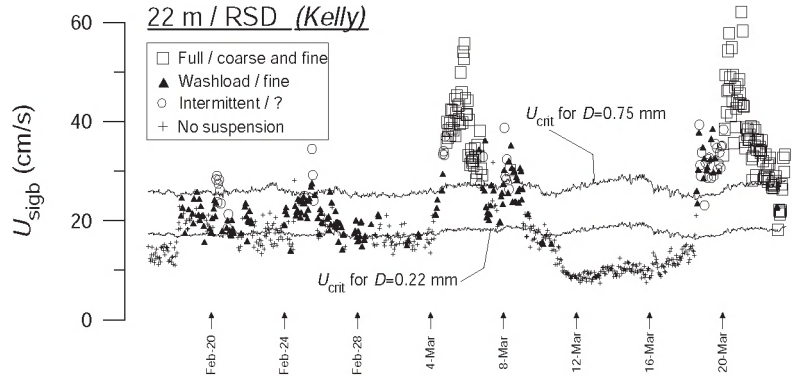

Fig. 6. U_{sigb} classified according to whether suspension over the RSD (*Kelly*, 22-m depth) at the time was full, intermittent, washload or nonexistent.

sand in the washload was resuspended from the adjacent fine-sand plain and advected across the RSD at times when the coarse bed sediment in the RSD itself was not in motion. Intermittent suspension tends to straddle U_{crit} based on $D = 0.75$ mm (Fig. 5). It is not clear what grain size composed the intermittent suspension. On the one hand, the burst-averaged concentration estimates $\bar{C}_{coarse}(z)$ during intermittent suspension were all at the ABS background noise level, which implies no coarse sand present. On the other hand, inspection of raw ABS data revealed short bursts of high concentration originating at the bed, which implies resuspension of the local (i.e., coarse) bed material. Another line of thinking also suggests the presence of coarse sand during intermittent suspension, as follows. There appears to be a hysteresis in coarse-sand suspension at the RSD: note in Fig. 6 that full suspension (which is always composed of coarse and fine sand) appears to begin at a higher U_{sigb} than it appears to cease. However, that hysteresis (i.e., coarse sand appearing in suspension at a higher orbital speed than it disappears from suspension) is seen to largely disappear if the intermittent suspension is composed of coarse as well as fine sand.

4.3. Burst-averaged suspension

Table 3 shows a summary of results regarding the burst-averaged fine- and coarse-sand concentration profiles, which can be referred to

Table 3
Summary of observations

	Suspended fine sand		Suspended coarse sand	
	Background swell	High waves	Background swell	High waves
	Suspension over the RSD			
Coarse-sand RSD/22-m depth	Large ripples.	Hummocky bed? Large ripples?	Large ripples.	Hummocky bed? Large ripples?
Kelly	Nonequilibrium C_0, implies nonlocal source (washload).	Flow-contraction term uses $\sigma = 0$ and $\Lambda = \infty$, and: (1) $D = 0.22$ mm… Nonequilibrium C_0, implies nonlocal source. (2) $D = 0.75$ mm… $C_0 = 0.005\rho_s\theta''^3$, implies local exhumation of fines.	No coarse sand in suspension.	$C_0 = 0.005\rho_s\theta''^3$, where flow-contraction term uses $\sigma = 0$ and $\Lambda = \infty$.
	Uniform profile.	Uniform profile.		Linear K_z, van Rijn β.
	Fine-sand suspension over fine-sand bed		*Coarse-sand suspension over fine-sand bed*	
Fine-sand plain/22-m depth	Rippled bed.	Hummocky bed.	Rippled bed.	Hummocky bed.
Alice	$C_0 = 0.005\rho_s\theta''^3$, where flow-contraction term uses σ, Λ = ripple dimensions.	$C_0 = 0.005\rho_s\theta''^3$, where flow-contraction term uses $\sigma = 0$ and $\Lambda = \infty$.	No coarse sand in suspension.	Nonequilibrium C_0, implies nonlocal source.
	Constant K_z	Linear K_z, Van Rijn β.		Linear K_z, van Rijn β.
	Ripple/hummock hysteresis?		Ripple/hummock hysteresis?	
Fine-sand plain/15-m depth	Rippled bed.	Hummocky bed.	Rippled bed.	Hummocky bed.
Bud	$C_0 = 0.005\rho_s\theta''^3$, where flow-contraction term uses σ, Λ = ripple dimensions.	$C_0 = 0.005\rho_s\theta''^3$, where flow-contraction term uses $\sigma = 0$ and $\Lambda = \infty$.	No coarse sand in suspension.	No coarse sand in suspension.
	Constant/linear K_z, van Rijn β.	Linear K_z, van Rijn β.		
	Ripple/hummock hysteresis?		Ripple/hummock hysteresis?	

throughout the following discussion. C_0 is the time averaged suspended-sediment reference concentration, which is specified at the level $z = 0$ cm. C_0 was obtained by fitting a straight line to $\log_{10}(\bar{C})$ versus z over the domain $1\,\text{cm} < z < 5\,\text{cm}$ and extrapolating the fitted line to $z = 0$ cm.

4.3.1. Fine-sand suspension over fine-sand bed

At both of the fine-sand sites (*Alice*, 22-m depth, and *Bud*, 15-m depth), the fine-sand suspension data (full and intermittent suspensions) tend to fall into two clusters when plotted in C_0-versus-θ' space. One cluster is described by the model $C_0 = 0.10\rho_s\theta'^3$ and the other by $C_0 = 0.005\rho_s\theta'^3$ (see top left panel in Figs. 7A and B). Here, θ' is the dimensionless wave-induced skin friction:

$$\Theta' = (0.5\rho f'_w U^2_{sigb})/[(\rho_s - \rho)gD], \quad (3)$$

where ρ_s is the sediment density (assumed to be $2.65\,\text{g/cm}^3$), ρ is water density, g is acceleration due to gravity and f'_w, the skin-friction wave-friction factor, is given by Swart (1974) as:

$$f'_w = \exp[5.213(k_s/d_{sigb})^{0.194} - 5.977], \quad (4)$$

where $k_s = 2.5D$ is the Nikuradse (grain) roughness and $d_{sigb} = TU_{sigb}/2\pi$.

Green and Black (1999) found a similar clustering of reference-concentration estimates from another New Zealand wave-dominated shoreface (Mangawhai, on the northeast coast of the North Island). By examining video observations of the seabed and suspension process that were acquired at the same time the ABS data were acquired, they were able to relate the clusters to the existence of two distinct bedform types, these being a rippled bed and a hummocky bed (Table 4 provides a summary). Green and Black found that the hummocky bed replaced the rippled bed when θ' exceeded approximately 0.14. They did not observe how the rippled bed reformed under decaying waves.

The Tairua fine-sand reference concentrations over the two fine-sand beds (15- and 22-m depth) fall into the same two clusters in C_0-versus-θ' space as the Mangawhai data, which suggests that the rippled and hummocky beds observed at Mangawhai also occurred at Tairua. However, $\theta' = 0.14$ does not adequately demarcate the two bedform types/data clusters for the Tairua dataset (top left panel in Figs. 7A and B). Instead, the rippled bed appears to occur under the background swell, and is replaced by the hummocky bed when U_{sigb} exceeds 35–45 cm/s (bottom panel in Figs. 7A and B). This range of values is significantly higher than U_{crit}, but note that the rippled bed apparently does not become re-established until U_{sigb} falls back towards U_{crit} (bottom panel in Figs. 7A and B).

Green and Black (1999) found that it was possible to collapse the Mangawhai reference-concentration data onto a single model by accounting for flow contraction in the wave boundary layer. This was achieved by using θ'' in place of θ' to describe the near-bed flow:

$$\Theta'' = (0.5\rho f'_w U^2_{sigb})/\{[(\rho_s - \rho)gD](1 - \pi\sigma/\Lambda)^2\}, \quad (5)$$

where σ is the ripple height and Λ is the ripple length, which resulted in all of the reference-concentration data collapsing onto the single model:

$$C_0 = 0.005\rho_s\Theta''^3. \quad (6)$$

Note that Green and Black used $\sigma =$ zero and $\Lambda = \infty$ for the hummocky bed, which has the effect of negating or "disabling" the flow-contraction correction. They defended this choice by arguing that because sediment was entrained principally from hummock slopes as a sheet flow, rather than from ripple crests under locally accelerated flow, the flow-contraction correction was not needed for the hummocks.

The Tairua fine-sand reference-concentration data over the fine-sand beds (15- and 22-m depth) also collapse onto Eq. (6) (top right panel in Figs. 7A and B). For the background-swell data, the figures given in Table 1 for σ and Λ were used in Eq. (5) to estimate θ''. Note, these are ripple dimensions determined from sidescan-sonar surveys of the Tairua shoreface conducted during fairweather ($U_{sigb} < U_{crit}$). For the hummocks that are presumed to form under high waves, σ was assumed to be zero and Λ was assumed to be infinite, following Green and Black (1999).

In addition to governing the relationship between bed shear stress and erosion of the seabed, the seabed shape—rippled or hummocky—also

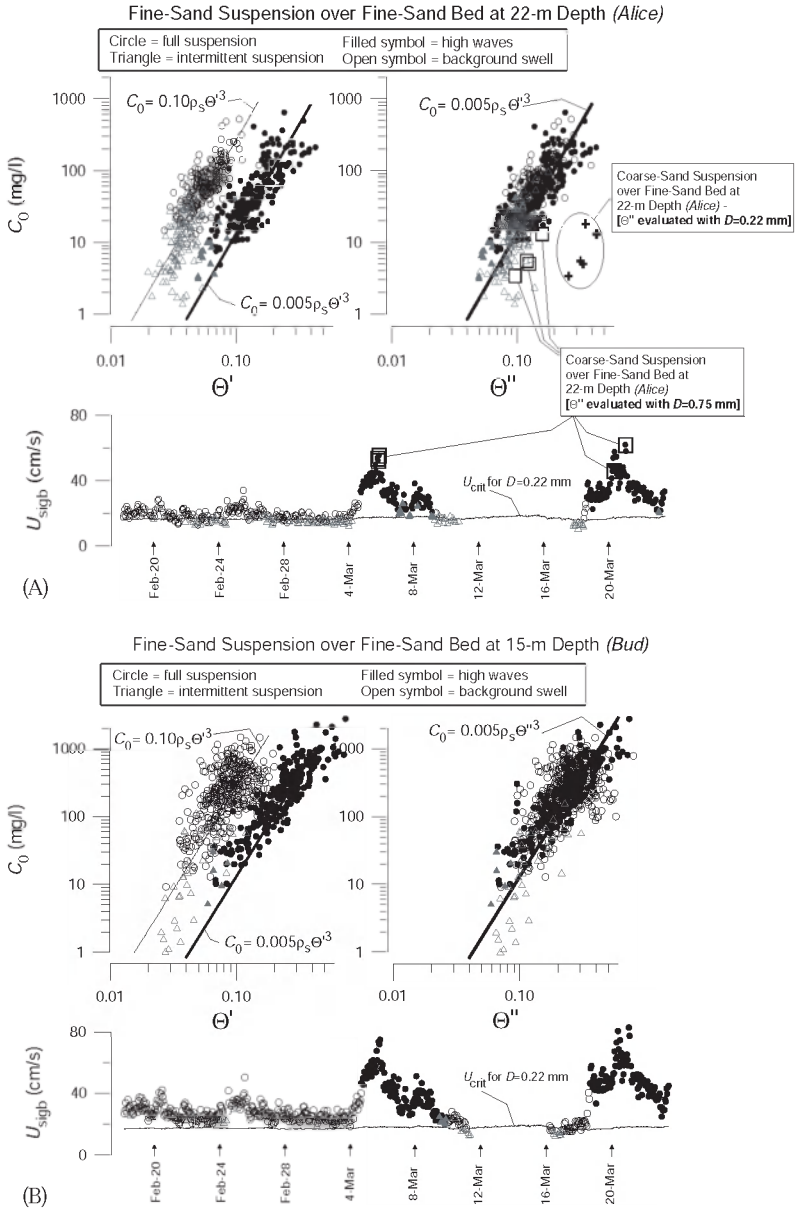

Fig. 7. Fine-sand reference concentration over fine-sand bed at: (A) 22-m depth and (B) 15-m depth. Refer to text for explanation.

appears to control the mixing of suspended fine sand close to the bed, as follows. Starting from the assumption that there is an exact balance at every level in the flow between time-averaged settling flux $\bar{C}w_s$ (where w_s is sediment settling speed) and turbulent diffusion $K(\partial\bar{C}/\partial z)$ (where K is sediment diffusivity), sediment diffusivity can be estimated from the concentration data as:

$$K = \bar{C}w_s/(\partial\bar{C}/\partial z). \quad (7)$$

Shown in Fig. 8 are two values of r^2, one value being for the fit of K between 1 and 20 cm above the bed to one model, and the other value being for the fit of K over the same range to another model.

Table 4
Bedforms observed by Green and Black (1999) on the wave-dominated shoreface at Mangawhai, New Zealand, and the associated suspension process and models that described the relationship between reference concentration and wave-induced skin friction

	Rippled bed	Hummocky bed
Bedform characteristics	Symmetrical, with rounded crests and troughs surmounting otherwise level seabed	Large-scale irregular deformation of the seabed
Bedform dimensions	Height 1–3 cm Length 10–20 cm	"Height" 10–20 cm "Length" 1–2 m
Suspension process	Suspension "carpet"	Sheet flow-bursting sequence
Reference concentration model, $C_0 = f(\theta')$	$C_0 = 0.10\rho_s\theta'^3$	$C_0 = 0.005\rho_s\theta'^3$
Reference concentration model, $C_0 = f(\theta'')$	$C_0 = 0.005\rho_s\theta''^3$	$C_0 = 0.005\rho_s\theta''^3$

The data were from two depths (7 and 12 m), both with seabed composed of well-sorted fine sand ($D = 0.23$ mm).

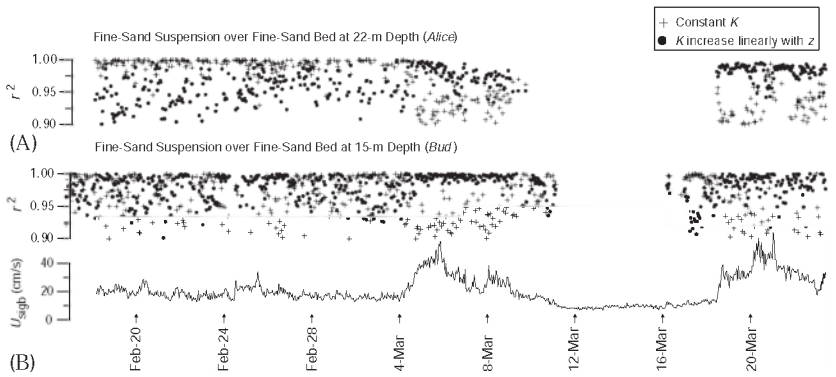

Fig. 8. r^2 for fit of measured K profile (fine sand) to the constant-K model and to the linearly increasing-K model: (A) 22-m depth and (B) 15-m depth.

The two models are: constant K, and K increasing linearly with elevation above the bed, where K was evaluated from Eq. (7) with $w_s = 2.2\,\mathrm{cm\,s^{-1}}$ (Stokes settling speed for grain size 0.22 mm). At the deeper of the two fine-sand sites (22-m depth, *Alice*), it is particularly clear that r^2 for the constant-K model exceeds r^2 for the linearly increasing-K model during background swell, when the bed was presumed to be rippled, but the converse is the case (the linearly increasing-K model fits the data better) for the period of high waves, when the bed was presumed to be hummocky. At the shallower site (15-m depth, *Bud*), the linearly increasing-K model is also clearly the better model for the presumed hummocky bed. However, the two values of r^2 tend to alternate during background swell, such that the constant-K model is the better fit when the waves are slightly smaller, and the linearly increasing-K model is the better fit when the waves are slightly larger. This observation suggests that there are not in fact two different shapes of the sediment-diffusivity profile, as follows.

The commonly accepted model for linearly increasing K is:

$$K = \beta\kappa U_* z, \tag{8}$$

where U_* is a characteristic friction velocity, κ is von Karman's constant and β is an empirical constant such that $\beta = K/K_m$, where K_m is momentum diffusivity and

$$\beta = 1 + 2[(w_s/U_*)^2] \tag{9}$$

is proposed by van Rijn (1993) as being applicable to steady flow. Using Eq. (9) for β with $w_s = 2.2\,\mathrm{cm\,s^{-1}}$ (fine sand), $\beta\kappa U_*$ is seen to

decrease for decreasing U_* over the range of friction velocities encountered during the background swell, even though β increases (Fig. 9). (Here, the characteristic friction velocity is taken as $U_* = (0.5 f_w U_{sigb}^2)^{1/2}$, which is the wave-induced friction velocity, with f_w given by Eq. (4) and k_s in that equation set at the ripple roughness $28\sigma^2/\Lambda$ (Grant and Madsen, 1982) (Table 1) to reflect wave-induced mixing in the near-bed region). Hence, the slope of the linearly increasing sediment-diffusivity profile reduces with decreasing U_*, such that the profile could become indistinguishable from a constant value. This behaviour may explain the observed alternation of r^2 at the 15-m site under background swell, with the apparent appearance of constant sediment diffusivity under low waves.

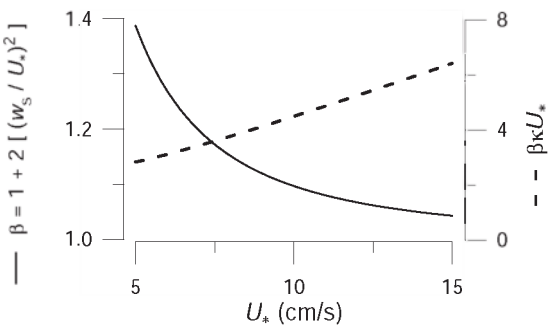

Fig. 9. β (Eq. (9), with $w_s = 2.2\,\mathrm{cm\,s^{-1}}$, which is the Stokes settling speed for grain size 0.22 mm) and $\beta\kappa U_*$ (the slope of the linearly increasing sediment-diffusivity profile) plotted against U_*.

Values of β for the fine-sand suspensions over the fine-sand beds (22-m depth, *Alice*, and 15-m depth, *Bud*) are shown in Fig. 10 together with Eq. (9). There is one value of β per burst, where $\beta = X/\kappa U_*$ and $U_* = (0.5 f_w U_{sigb}^2)^{1/2}$, as above. Here, X is the slope of the straight line fitted to K versus z over the domain $1\,\mathrm{cm} < z < 20\,\mathrm{cm}$, where K was estimated as described previously. The values of β for the fine-sand suspensions over the fine-sand beds (15-m depth and 22-m depth) scatter widely around Eq. (9).

4.3.2. *Coarse-sand suspension over fine-sand bed*

The reference concentration for the suspended coarse sand that appeared at the 22-m fine-sand site at times of highest waves tended to plot just below the model $C_0 = 0.005\rho\theta''^3$, which was applicable to the suspended fine sand at those same times (top right panel in Fig. 7A). Note that,

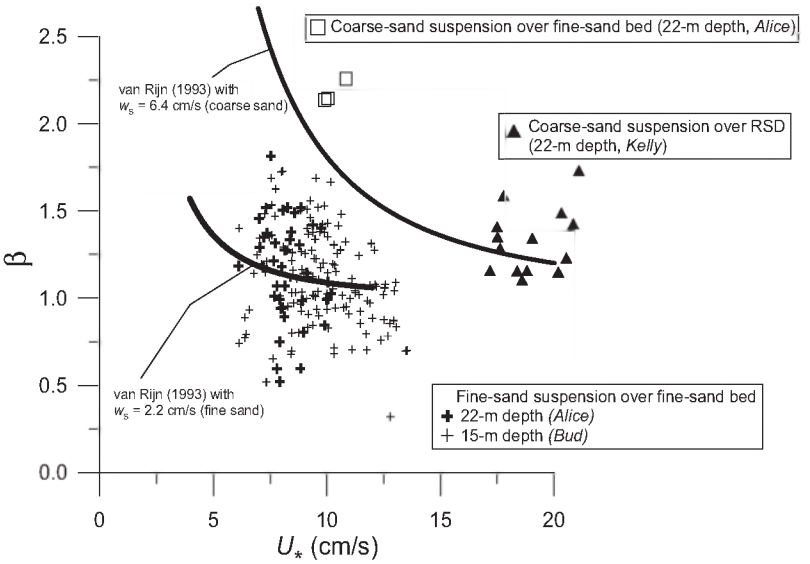

Fig. 10. Observed and predicted β. Observed values are shown only for bursts for which r^2 for the fit of the straight line to K versus z over the domain $1\,\mathrm{cm} < z < 20\,\mathrm{cm}$ exceeds 0.99.

for the case of coarse-sand suspended over the fine-sand bed, it is not clear what grain size should be used to evaluate dimensionless wave-induced skin friction (either θ'' or θ'). For the coarse-sand data points shown in the top right panel of Fig. 7A that plot just below the model $C_0 = 0.005\rho\theta''^3$, θ'' was evaluated with $D = 0.75$ mm (i.e., coarse sand). Also shown in the top right panel are the coarse-sand data points with θ'' evaluated with $D = 0.22$ mm (i.e., fine sand); these data points plot well below the model $C_0 = 0.005\rho\theta''^3$.

A possible explanation for the smaller-than-predicted coarse-sand reference concentrations is that the source of the suspended coarse sand, assuming it was the RSD, was distant and therefore the suspended coarse sand was not "in equilibrium" with the local bed material. In mechanistic terms, this means that there could be no continuous exchange of bed and suspended particles that normally maintains an equilibrium suspension, with the result that the suspension gradually dwindles as it moves farther from its source material.

K for the coarse sand (inferred from the coarse-sand concentration profiles using Eq. (7) with $w_s = 6.4\,\mathrm{cm\,s^{-1}}$, which is the Stokes settling speed for $D = 0.75$ mm) increased linearly with increasing z, which was also the case for the fine sand in suspension at the same time. Values of β for the coarse sand are shown in Fig. 10 together with predicted values by Eq. (9). The observed values are somewhat larger than the predicted values.

4.3.3. Suspension over the RSD

During full suspension under high waves at the RSD (*Kelly*, 22-m depth), both coarse and fine sand was always in suspension.

The high-wave coarse-sand reference-concentration data plotted on the model $C_0 = 0.005\rho\theta'^3$ (not shown in a plot) (where θ' was evaluated with $D = 0.75$ mm, i.e., coarse sand), hence the data can only collapse onto the model $C_0 = 0.005\rho\theta''^3$ by assuming σ is zero and Λ is infinite in order to effect the transformation of θ' into θ'' (Fig. 11). The obvious inference is that sediments within the RSD evolved into a hummocky bed under high waves, in exactly the same way that the ripples on the surrounding fine-sand plain were inferred to

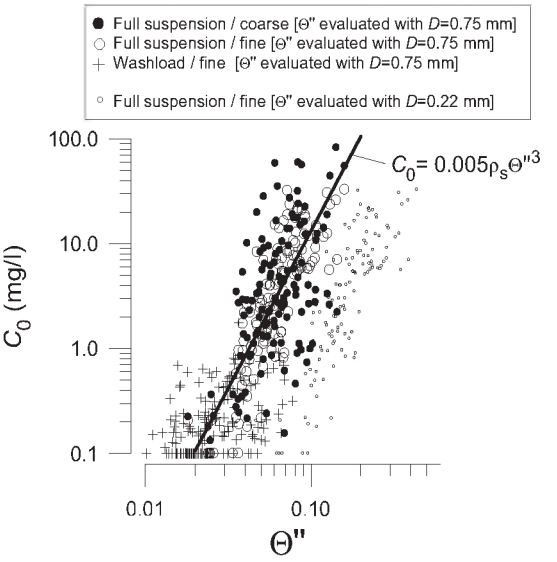

Fig. 11. Coarse-sand, fine-sand and washload reference concentrations over the RSD (*Kelly*, 22-m depth). θ'' is evaluated with σ = zero and $\Lambda = \infty$.

evolve into hummocks under high waves. Another possibility, however, is that sediment was entrained principally as sheet flow from the relatively larger ripples of the RSD, which, referring back to Green and Black's (1999) argument presented earlier, negates the need for the flow-acceleration correction. Without direct observations of the RSD bedforms under high waves, we cannot know which, if either, is correct. It should be noted, however, that from a process point of view, sheet-flow entrainment from hummocks and sheet-flow entrainment from prominent ripples are, of course, the same.

The high-wave fine-sand reference-concentration data plot well below the model $C_0 = 0.005\rho\theta''^3$ when θ'' is evaluated with $D = 0.22$ mm (i.e., fine sand) (Fig. 11). Thus, the explanation that was developed for the smaller-than-predicted coarse-sand reference concentration over the fine-sand bed can be applied here, too: the smaller-than-predicted fine-sand reference concentration over the coarse-sand bed is due to the suspended fine sand not being in equilibrium with the local (i.e., coarse) bed material of the RSD. However, if θ'' is evaluated with $D = 0.75$ mm, (i.e., coarse

sand), then the fine-sand reference-concentration data plots, together with the coarse-sand data, on the model $C_0 = 0.005\rho\theta''^3$ (Fig. 11). This suggests an equilibrium suspension, which in turn suggests that fine sand might be exhumed from within the RSD when high waves mobilise the RSD coarse sand (and when hummocks appear?), thus enabling sustenance of an equilibrium fine-sand suspension over the RSD at those times. It is not clear, from this dataset, which possibility (nonlocally sourced, nonequilibrium suspension or equilibrium suspension fed by exhumation of local fine source material), if either, is correct.

Under high waves at the RSD, fine sand was mixed uniformly throughout the near-bed region, and therefore it was not possible to estimate a corresponding value for the sediment diffusivity (because $\partial\bar{C}_{\text{fine}}/\partial z = 0$). Presumably, when waves were large, the diffusivity of the fine sand (low settling velocity) over the rough bed of the RSD was high, which of course is consistent with a uniform concentration profile. On the other hand, K for the coarse sand suspended over the RSD during high waves increased linearly with elevation above the bed, and the value of β inferred from the data (assuming $w_s = 6.4\,\text{cm s}^{-1}$) compared favourably with van Rijn's (1993) model (Fig. 10).

The reference concentration of the washload, which was always composed entirely of fine sand and which appeared over the RSD when U_{sigb} was greater than U_{crit} based on $D = 0.22\,\text{mm}$ but less than U_{crit} based on $D = 0.75\,\text{mm}$ (Fig. 6), plots with large scatter in Fig. 11. Previously, we suggested that the source area for the washload was the fine-sand plain that is adjacent to the RSD. Reasoning from the equilibrium argument presented previously, if that is the case then the washload over the RSD would not have been in contact with its source area, which might explain the scatter in Fig. 11.

5. Discussion—inhibited deposition of fine sands on coarse beds

The fine sand observed in suspension over the Tairua RSD under both background swell and high waves was always uniformly mixed (see Table 3 for summary of observations) throughout at least the bottom meter of the water column, which suggests a high level of turbulent mixing. Although this will not prevent deposition of fine sand, it is indicative of an unfavourable settling environment, which supports Murray and Thieler's (2003) choice of mechanism (i.e., inhibited deposition of fine sand over coarse domains) at the heart of the positive feedback that causes sorted bedforms (i.e., RSDs) to self-organize. Other insights can be developed from further analysis of the Tairua dataset, as follows.

Under the long-period background swell that preceded the first high-wave event, fine sand was in almost continuous suspension on the fine-sand plain that surrounded the RSD at 22-m depth. For $U_{\text{sigb}} \approx U_{\text{crit,fine}}$ (where $U_{\text{crit,fine}}$ is critical wave-orbital speed at the bed for initiation of suspension of fine sand), SSC over the Tairua RSD was zero, even though fine sand was in suspension over the surrounding fine-sand plain. Taking for granted the existence of an advecting current, the simplest explanation for this observation is that the fine sand sourced from the surrounding plain settled to the bed (of the RSD) before reaching the measurement location (in the interior of the RSD). Hence, fine sands can settle on the RSD, which is consistent with the observation that sediments of the Tairua RSD are poorly sorted mixtures of fine and coarse sand (Hume et al., 2003).

It follows that as U_{sigb} becomes larger (resuspending a greater quantity of sand on the fine-sand plain) and/or the advecting current becomes stronger, suspended fine sand will penetrate farther into the interior of the RSD. The data support this conjecture: for $U_{\text{sigb}} > U_{\text{crit,fine}}$, fine sand appeared at the measurement location in the interior of the RSD in a washload. Although the uniform fine-sand suspension profile that is characteristic of the washload is indicative of inhibited settling, deposition of fine sand on the RSD may still occur.

The Tairua RSD thus cannot be a static patch of coarse material that resolutely resists the intrusion of fine sand from the surrounding fine-sand plain. Under high waves, the suspended-sediment load impinging from the surrounding plain will be

correspondingly high, but turbulence will also be correspondingly more energetic on the RSD, thus more effectively inhibiting deposition. Under low waves, deposition may be less inhibited on the RSD, but the suspended-sediment load arriving from the surrounding fine-sand plain will also be lower. Thus, the fine-sand deposition rate on the RSD will be small, even though conditions are more favourable for settling.

On a wave-dominated shelf, the wave-orbital speed at the bed is the principal control on sediment resuspension as well the "level" (energy) of turbulence. In this case, at any particular water depth, as waves get higher, more bed sediment is entrained and the potential for RSD burial increases (simply because there is more sediment in suspension that has to eventually settle somewhere). However, at the same time, turbulence levels generally increase. It is not clear whether turbulence levels would increase faster over the rougher bed of an RSD, but, either way, the ability of the RSD to cleanse itself of fine sand would also increase. This kind of thinking suggests the possibility of a balance between RSD burial and persistence, mediated by wave climate. For instance, under a wave climate characterised by long periods of competent (i.e., able to resuspend bed sediment) but low waves, whenever fine sand is in suspension, turbulence over any incipient RSD might be weak, and hence the incipient RSD may not be very effective at inhibiting deposition of that suspended fine sand on itself. In this case, the incipient RSD, which is small, might be obliterated by the slow burial processes under the low waves before it has a chance to grow. On the other hand, on a shelf where waves are either incompetent or very high, whenever fine sand is in suspension and burial potential is high, turbulence over any incipient RSD would also be strong. In this case, incipient RSDs might grow and coalesce to form large, stable features. Hence, some wave climates might promote the formation of RSDs, and others might suppress their growth. If that is so, then water depth would play a similar role, since orbital motions are attenuated by water depth, which controls the way in which the surface wave climate is transformed into a "seabed wave climate". Therefore, a more accurate conclusion is that some combinations of (surface) wave climate and water depth might promote the formation of RSDs, and other combinations might suppress their growth. An additional factor that is likely to be important is sediment supply and availability.

Murray and Thieler's (2003) self-organization model is founded on an inhibited deposition of fine sediments, not zero deposition. This distinction is important, since it implies that RSDs are not guaranteed to persist, which is necessary since buried RSDs have been observed on a number of shelves (Hunter et al., 1988; Thieler et al., 2001; Hume et al., 2003). Consideration of the balance between inhibition of settling and the tendency for burial by the sediment load that impinges from the shelf surrounding an RSD leads to a focus on wave climate and water depth as possible "mediators" of the basic self-organization process. The existence of such balances, which might tip first one way and then another under a typical variable wave climate, further reinforces the view that RSDs are not static, palimpsest, features, which is consistent with the sedimentological evidence of downdrift migration and interfingering of strata around the edges of RSDs (e.g., Thieler et al., 2001). Further modelling taking into account factors such as the role of wave climate might shed some light on how these balances are played out and whether there are indeed combinations of wave climates and water depths that either promote or suppress the formation of RSDs on wave-dominated shelves.

Another possibility is that flux coupling plays a role. Fine sand would be inhibited from accumulating on the RSD if flux coupling were suitably larger over the RSD compared to over the fine-sand plain at the same time. This seems unlikely during periods of background swell at Tairua, since the fine sand appeared in suspension over the RSD at those times as a washload, which was characterised by virtually zero intermittency at both the individual-wave and wave-group scales. Hence, the flux-coupling can be expected to be small or zero. Suspension under high waves at the Tairua RSD was intermittent, which might translate into a larger flux coupling compared to under background swell. A detailed analysis of the flux

coupling term might therefore shed some further light on how RSDs are maintained.

Finally, it seems that coarse sand entrained from the RSD does escape onto the surrounding fine-sand plain, as evidenced by the nonequilibrium coarse-sand suspension that developed over the fine-sand bed adjacent to the RSD during periods of high waves. Dispersal of coarse sand in this way may be the metaphorical equivalent of throwing out "seeds" that can grow into RSDs, given the right water depth and a favourable sequence of waves over a period of time.

6. Conclusions

The Tairua dataset provides insights into the comparative resuspension of fine and coarse sands by waves on this shoreface. Sediment suspension shows changes through time as wave conditions change (changes in bedforms, changes in entrainment, changes in mixing), differences with substrate (e.g., vortex entrainment of fine-sand on open plains versus fine-sand "washload" over RSDs), and differences with depth (cross-shelf variation in intermittency at the wave scale). In addition, there appear to be subtle effects such as a hysteresis in the way bedforms evolve, nonequilibrium sediment loads, and possibly exhumation of fine sediments from within RSDs.

Intermittency at the wave scale showed differences between depths (more intermittent at greater depth) and between seabed types at the same depth (vortex entrainment more pronounced over the fine-sand plain compared to over the RSD at 22-m depth). Detailed analysis of flux coupling at the wave scale is out of the scope of this paper, however, these observations suggest that there will be marked differences in flux coupling with depth and substrate. Although flux coupling may give rise to a minor term in the transport budget, such differences might be significant in the sediment-flux divergence and, hence, evolution of the shoreface morphology. Flux coupling may also play a role in maintenance of the RSDs. Flux coupling therefore merits further attention.

Table 3 provides a summary of features of the time-averaged suspended-sediment load, grouped by substrate and wave conditions. There is no obvious interaction between the fine and coarse suspensions. Hence, fine and coarse particles could be treated independently in a shelf sediment-transport model. In fact, most observations could be readily incorporated into a model, with a few notable exceptions. Firstly, the RSD needs to be explicitly incorporated into any such model, since it is a source of coarse material, as evidenced by the nonequilibrium coarse-sand suspension that appeared over the surrounding fine-sand plain under high waves. The RSD also has an effect on mixing of the fine-sand load that is sourced from the surrounding plain (fine sand is uniformly mixed over the RSD during times of background swell and high waves), which might affect settling of fine sand on the RSD and patterns of fine-sand transport. Secondly, bedforms need to evolve with the wave conditions to capture ripple–hummock transformations, which might include a hysteresis in the construction of a rippled bed under decaying waves. This is required because the seabed configuration is a first-order control on the relationship between wave-induced skin friction and reference concentration, and may also control the sediment diffusivity, although that is less clear. Finally, exhumation of fine sand from within the RSD might need to be accounted for in any model.

Suspended fine sand encounters an unfavourable settling environment over the RSD, which Murray and Thieler (2003) hypothesised was at the heart of a positive feedback that causes RSDs to self-organize from initial perturbations. The Tairua data suggest the possibility of a balance between RSD burial and the tendency to self-organize, mediated by wave climate and constrained by water depth. Furthermore, escape of coarse sand from RSDs under high waves may seed the growth of new RSDs.

Acknowledgements

Funded by the NZ Foundation for Research, Science and Technology (C01X0218) and the US National Science Foundation (INT-9987936). We thank L.D. Wright for comments and inspiration, and Rod Budd, Rick Liefting, John Hawken,

Bob Gammisch, Todd Nelson, Wayne Reisner and Grace Battisto for assistance in the field.

References

Bagnold, R.A., 1946. Motion of waves in shallow water: interaction of waves and sand bottoms. Proceedings of the Royal Society of London, Series A 187, 1–15.

Bradshaw, B.E., Healy, T.R., Nelson, C.S., Dell P, M., de Lange, W.P., 1994. Holocene sediment lithofacies and dispersal systems on a storm-dominated, back-arc shelf margin: the east Coromandel coast, New Zealand. Marine Geology 119, 75–98.

Cacchione, D.A., Drake, D.E., 1982. Measurements of storm-generated bottom stress on the continental shelf. Journal of Geophysical Research 87, 1952–1960.

Cacchione, D.A., Drake, D.E., Grant, W.D., Tate, G.B., 1984. Rippled scour depressions on the inner continental shelf off central California. Journal of Sedimentary Petrology 54 (4), 1280–1291.

Carter, L., Heath, R., 1975. Roles of mean circulation, tides, and waves in transport of bottom sediment on the New Zealand continental shelf. New Zealand Journal of Marine and Freshwater Research 9, 423–448.

Crawford, A.M., Hay, A.E., 1993. Determining suspended sand size and concentration from multi-frequency acoustic backscatter. Journal of the Acoustics Society of America 94, 3312–3324.

Gorman, R.M., Bryan, K., Laing, A.K., 2003. A wave hindcast for the New Zealand region—nearshore validation, coastal wave climate. New Zealand Journal of Marine, Freshwater Research 37 (3), 567–588.

Grant, W.D., Madsen, O.S., 1982. Moveable bed roughness in unsteady oscillatory flow. Journal of Geophysical Research 87, 469–481.

Green, M.O., 1999. Test of sediment initial-motion theories using irregular-wave field data. Sedimentology 46, 427–441.

Green, M.O., Black, K.P., 1999. Suspended-sediment reference concentration under waves: field analysis and critical analysis of two predictive models. Coastal Engineering 38, 115–141.

Green, M.O., MacDonald, I.T., 2001. Processes driving estuary infilling by marine sands on an embayed coast. Marine Geology 178, 11–37.

Green, M.O., Vincent, C.E., McCave, I.N., Dickson, R.R., Rees, J.M., Pearson, N.D., 1995. Storm sediment transport: observations from the British North Sea shelf. Continental Shelf Research 15, 889–912.

Hanes, D.M., Huntley, D.A., 1986. Continuous measurements of suspended sand concentration in a wave dominated nearshore environment. Continental Shelf Research 6, 585–596.

Hume, T.M., Trembanis, A.C., Wright, L.D., Hill, A., Liefting, R.M., 2003. Spatially variable, temporally stable, sedimentary facies on an energetic inner shelf. In: Coastal Sediments 2003. American Society of Civil Engineers, New York.

Hunter, R.E., Dingler, J.R., Anima, R.J., Richmond, B.M., 1988. Coarse-sediment bands on the inner shelf of Monterey Bay, California. Marine Geology 80, 81–98.

Huntley, D.A., Hanes, D.M., 1987. Direct measurement of suspended sediment transport. In: Kraus, N.C., (Ed.), Coastal Sediments '87, Vol. 1. American Society of Civil Engineers, New York, pp. 723–733.

Jaffe, B.E., Sternberg, R.W., Sallenger, A.S., 1985. The role of suspended sediment in shore-normal beach profile changes. In: Edge, B.L., (Ed.), Proceedings of the 19th International Coastal Engineering Conference, Vol. 2. American Society of Civil Engineers, New York, pp. 1983–1996.

Karl, H.A., 1980. Speculations on the processes responsible for mesoscale current lineations in the continental shelf, southern California. Marine Geology 34, M9–M18.

Komar, P.D., Miller, M.C., 1975. On the comparison between the threshold of sediment motion under waves and unidirectional currents with a discussion of the practical evaluation of the threshold. Journal of Sedimentary Petrology 45, 362–367.

Longuet-Higgins, M.S., 1975. On the joint distribution of periods and amplitudes of sea waves. Journal of Geophysical Research 80, 2688–2694.

Madsen, O.S., Wright, L.D., Boon, J.D., Chisholm, T.A., 1993. Wind stress, bed roughness and sediment transport on the inner shelf during an extreme storm event. Continental Shelf Research 13, 1303–1324.

Murray, A.B., Thieler, E.R, 2003. A new hypothesis for the formation of large-scale inner-shelf sediment sorting and "rippled scour depressions". Continental Shelf Research, submitted.

Niedoroda, A.W., Swift, D.J.P., Hopkins, T.S., Ma, C.-M., 1984. Shoreface morphodynamics on wave-dominated coasts. Marine Geology 60, 331–354.

Reimnitz, E., Toimil, L.J., Shepard, F.P., Gutierrez-Estrado, M., 1976. Possible rip-current origin for bottom ripple zones to 30-m depth. Geology 4, 395–400.

Shi, N.C., Larsen, L.H., 1984. Reverse sediment transport induced by amplitude-modulated waves. Marine Geology 54, 181–200.

Sleath, J.F.A., 1982. The suspension of sand by waves. Journal of Hydraulic Research 20, 439–452.

Storlazzi, C.D., Jaffe, B.E., 2002. Flow and sediment suspension events on the inner shelf of central California. Marine Geology 181, 195–213.

Swart, D.H., 1974. Offshore Sediment Transport and Equilibrium Beach Profiles. Publ. 131, Delft Hydraulics Lab., Delft, The Netherlands, 315pp.

Thieler, E.R., Brill, A.L., Cleary, W.J., Hobbs, C.H., Gammisch, R.A., 1995. Geology of the Wrightsville Beach, North Carolina shoreface: implications for the concept of shoreface profile of equilibrium. Marine Geology 126, 271–287.

Thieler, E.R., Pilkey, O.H., Cleary, W.J., Schwab, W.C., 2001. Modern sedimentation on the shoreface and inner

continental shelf at Wrightsville Beach, NC, USA. Journal of Sedimentary Research 71, 958–970.

Thorne, P.D., Hanes, D.M., 2002. A review of acoustic measurement of small-scale sediment processes. Continental Shelf Research 22, 603–632.

Thorne, P.D., Vincent, C.E., Hardcastle, P.J., Rehman, S., Pearson, N.D., 1991. Measuring suspended sediment concentrations using acoustic backscatter devices. Marine Geology 98, 7–16.

van Rijn, L.C., 1993. Principles of Sediment Transport in Rivers, Estuaries and Coastal Seas. Aqua Publications, Amsterdam.

Villard, P.V., Osborne, P.D., Vincent, C.E., 1999. Influence of wave groups on sand re-suspension over bedforms in a large-scale wave flume. In: Proceedings of the Coastal Sediments '99. ASCE, New York, pp. 367–376.

Vincent, C.E., Hanes, D.M., Bowen, A.J., 1991. Acoustic measurements of suspended sand on the shoreface and the control of concentration by bed roughness. Marine Geology 96, 1–18.

Williams, J.J., Rose, C.P., Thorne, P.D., O'Connor, B.A., Humphery, J.D., Hardcastle, P.J., Moores, S.P., Cooke, J.A., Wilson, D.J., 1999. Field observations and predictions of bed shear stresses and vertical suspended sediment concentration profiles in wave-current conditions. Continental Shelf Research 19, 507–536.

Wright, L.D., Boon, J.D., Green, M.O., List, J.H., 1986. Response of the mid-shoreface of the southern mid-Atlantic Bight to a 'northeaster'. Geo-Marine Letters 6, 153–160.

Wright, L.D., Boon, J.D., Kim, S.-C., List, J.H., 1991. Modes of cross-shore transport on the shoreface of the Middle Atlantic Bight. Marine Geology 96, 19–51.